Linking Retinal, Neural, and Perceptual Measures of Glaucoma with Diffusion Magnetic Resonance Imaging (dMRI)

Nathaniel Miller[a], Yao Liu[b,c], Roman Krivochenitser[b], and Bas Rokers[a,c]

a. Department of Psychology, University of Wisconsin-Madison

b. Dept. of Ophthalmology and Visual Sciences, University of Wisconsin School of Medicine and Public Health

c. McPherson Eye Research Institute, University of Wisconsin School of Medicine and Public Health

Funding: This research was funded in part by an institutional grant from Research to Prevent Blindness to the University of Wisconsin-Madison Dept. of Ophthalmology and Visual Sciences.

Acknowledgements: We thank Anna Bauman for assistance with patient recruitment and data collection and Franco Pestilli for comments that greatly improved the manuscript.

Abstract

Purpose: To link the clinically defined retinal and perceptual deficits in glaucoma by quantifying optic nerve structural integrity in the human visual system.

Methods: We characterized optic nerve (ON) neuropathy in patients with unilateral glaucoma (n = 6) using probabilistic diffusion weighted imaging (DWI) tractography.

Results: Glaucoma was associated with reduced structural integrity of the optic nerves. Specifically, we found reduced fractional anisotropy in the ONs of eyes with advanced, as compared to mild, stages of disease ($F(1,10) = 55.474$, $p < 0.00001$). Furthermore, by comparing the ratios of ON fractional anisotropies in glaucoma subjects to those of healthy controls (n = 6) we determined that this difference was beyond that expected from normal anatomical variation ($F(1,9) = 20.276$, $p < 0.005$). Finally, we linked neural integrity to clinical assessments. Retinal measures (vertical cup-to-disc ratio) predicted optic nerve neural integrity (ON FA) ($F(1,10) = 11.061$, $p < 0.01$), and neural integrity in turn predicted perceptual performance (visual field index (VFI)) ($F(1,10) = 15.308$, $p < 0.005$).

Conclusion: We provide methods to detect glaucoma-related structural changes in the optic nerves and establish that the retinal, neural, and perceptual measures of glaucoma are well-correlated.

Translational Relevance: We demonstrate the potential of diffusion MRI as a clinical tool in human glaucoma. Early detection is critical given the degenerative nature of the disease, and the availability of additional diagnostic tools such as dMRI may significantly improve treatment outcome.

Precis

Glaucoma is the leading cause of irreversible vision loss. Here we link clinical measures of optic nerve structure and function to diffusion magnetic resonance imaging (dMRI) measures of optic nerve integrity. These results will help improve the early diagnosis and treatment of glaucoma.

Introduction

Vision loss is a major cause of disability worldwide. Particularly common among the elderly, it confers a greater risk of injury and diminished quality of life.[1,2] Glaucoma is the leading cause of irreversible vision loss and is projected to affect nearly 80 million individuals by 2020.[3] It is clinically defined by characteristic patterns of visual field impairment, thinning of the retinal nerve fiber layer, and optic nerve damage.[4] There is growing evidence that glaucoma may be a neurodegenerative condition. Recent studies suggest that the pathogenesis of glaucoma bears similarities to that of Alzheimer's disease, Parkinson's, and amyotrophic lateral sclerosis (ALS).[6] Thus, research seeking to understand the possible underlying neurodegenerative processes associated with glaucoma may help guide the development of more robust treatment paradigms and have applications for improving our understanding of other neurodegenerative diseases. In addition, current glaucoma treatments are limited to the reduction of intraocular pressure (IOP) to prevent progressive visual field loss. However, many patients continue to lose vision despite treatment, and no treatments are available to reverse damage that has already occurred to the visual system.[4] Therefore, the development of new methods enabling earlier

diagnosis and more precise quantification of disease progression are essential to limiting neurodegenerative damage and improving patient outcomes.

Recent MRI-based *in vivo* human studies have used voxel-based morphometry (VBM) and diffusion tensor imaging (DTI) to explore gray- and white-matter cortical changes associated with glaucoma, and have shown reduced gray-matter (GM) volume in late stages of the disease, along with significant rarefaction along the optic radiations.[7,8,9] While these preliminary results are consistent with animal models and post-mortem pathological studies of human subjects,[10] there is a need for more precise evaluation of neurological changes, particularly at the level of the optic nerves. Animal model studies of the early visual system using diffusion MRI (dMRI) demonstrate the ability to detect changes in the neural integrity of the optic nerves from damage occurring within the retina, emphasizing the need for *in vivo* human study of this technique.[11,12]

In recent years, diffusion-weighted imaging (DWI) based probabilistic tractography methods have been developed to evaluate white-matter changes in the human visual system. This methodology has demonstrated significant findings in patients with amblyopia[13]. Its application in subjects with asymmetric glaucomatous optic neuropathy in each eye provides a unique opportunity to evaluate DWI methods as a diagnostic tool for visual disorders, linking changes in white matter integrity to structural and functional changes in glaucoma. Recent methodological advances make it possible to reliably identify the microstructural properties of the optic nerve.[14] Using a pair of diffusion scans acquired with opposite phase-encoding directions, a low-noise field-corrected volume can be created,[15,16] allowing the optic nerves to be isolated using probabilistic tractography. This affords the unique opportunity to precisely quantify changes in the visual system of glaucoma patients. Further, we purposefully selected patients with asymmetric glaucomatous optic nerve damage to allow for within-subjects comparisons of optic nerve properties, quantifying differences in eyes with “advanced” versus “mild” glaucoma.

We used an advanced DWI tractography method to identify and analyze the optic nerves of six asymmetric glaucoma patients and six controls. Using both within-subject analyses and comparison to controls, we evaluated structural changes in the optic nerves associated with glaucoma. Furthermore, we assessed the relationship between these MRI-based neural measures, measures of retinal integrity (e.g. vertical cup-to-disc ratio), and perceptual measures (e.g. visual field index (VFI)).

Methods

Participants

All work was carried out in accordance with the Code of Ethics of the World Medical Association (Declaration of Helsinki). Informed consent was obtained from all participants and all participants completed MRI screening with consultation and approval obtained from their physicians as needed to ensure they could safely participate.

Glaucoma Patients: Six glaucoma patients (4 female) aged 19-66 years (mean 53.3 ± 17.4) were recruited from the Glaucoma Service of the University of Wisconsin Hospitals and Clinics (Table 1). All patients had diagnoses of either primary open-angle, pigment dispersion, pseudoexfoliation, or chronic angle-closure glaucoma and had a history of elevated IOPs greater than 22 mmHg. Selection criteria included a best-corrected Snellen visual acuity of 20/25 or better in the eye with "mild" glaucoma and 20/200 or better in the eye with "advanced" glaucoma. Patients with normal/low-pressure glaucoma or any history of neurodegenerative diseases, diabetic retinopathy, advanced macular degeneration, uveitis, or previous (non-surgical) eye trauma were excluded.

Control Subjects: Control subjects were recruited from the University of Wisconsin-Madison. Six sex-matched subjects aged 21-34 years (mean 24 ± 5.3) were included in the analysis. All subjects had best corrected Snellen visual acuity of 20/20 or better and had no prior medical history of neurologic or ocular pathology other than refractive error. Eye dominance was determined using the "hole-in-the-card" test.

Participant Demographic and Ophthalmologic Information							
Participant	**Age**	**Sex**	**Eye**	**VA**	**VFI**	**vCD**	**RNFL (µm)**
G1	19	F	OD	20/20	100%	0.34	121
			OS	**20/30**	**41%**	**0.83**	**56**
G2	54	M	**OD**	**20/20**	**92%**	**0.66**	**66**
			OS	20/20	99%	0.63	70
G3	57	F	**OD**	**20/25**	**54%**	**0.82**	**52**
			OS	20/30	99%	0.63	73
G4	59	M	**OD**	**20/30**	**62%**	**0.82**	**45**
			OS	20/20	97%	0.80	57
G5	65	F	OD	20/40	96%	0.57	73
			OS	**20/25**	**69%**	**0.78**	**52**
G6	66	F	OD	20/20	100%	0.74	83
			OS	**20/20**	**91%**	**0.89**	**66**

Table 1. Characteristics of asymmetric glaucoma patients including age, sex, best corrected Snellen visual acuity (VA), visual field index (VFI), vertical cup-to-disc ratio (vCD), and average retinal nerve fiber layer thickness (RNFL). Eyes with advanced glaucoma are indicated in **bold**.

Clinical Measures

Clinical measures of optic nerve structure and function were assessed for each of the six patients during routine ophthalmologic exams by a glaucoma specialist (Y.L.). These measures included visual acuity (VA), vertical cup-to-disc ratio (vCD), average retinal nerve fiber layer thickness (RNFL), and visual field index (VFI). The vCD was determined by direct visualization of the optic nerve using slit-lamp biomicroscopy, average RNFL thickness was measured using Cirrus Spectral-Domain Optical Coherence Tomography (Carl Zeiss Meditec, Inc., Dublin, CA, USA) with all scans having adequate signal strength >7/10, and VFI was measured using the Humphrey visual field 24-2 SITA-Standard testing algorithm (Carl Zeiss Meditec, Inc. Dublin, CA, USA).

Magnetic Resonance Imaging Data Acquisition

Brain imaging data was obtained at the Waisman Center using a GE Discovery Medical 3T MRI scanner (GE Healthcare, Inc., Chicago, IL, USA) equipped with a 32-channel head coil. First, a 10-minute structural whole-brain T1-weighted anatomical scan (2.93 ms TE; 6.70 ms TR;

1 mm^3 isotropic voxels) was acquired. Then, a 15-minute diffusion sequence with two 48-direction diffusion-weighted scans (6 b_0), collected in the anterior to posterior (AP) and posterior to anterior (PA) directions (76.7 ms TE; 8.1 s TR; 2.0 mm^3 isotropic voxels; b = 2000 nm/s^2; reconstruction matrix FOV: LR 212 mm x AP 212 mm x FH 144 mm).

Data Processing

Pre-processing: To improve the quality of our tractography and increase the signal-to-noise ratio in the nasal cavity, the two reverse-encoded (AP and PA) diffusion scans were combined into a single corrected volume using FSL (University of Oxford, Oxford, England)[15,16]. Subsequent processing was completed using the mrVista software package (Stanford University, Stanford, California), based on previously published methods.[13] A mean *b=0* image was calculated from the corrected DTI volume and underwent eddy current correction. This corrected b_0 image was co-registered to the AC-PC-aligned T1 image and diffusion tensors were fit to the volume using a least-squares estimate bootstrapped 500 times[17].

ROI Placement: We manually identified three regions of interest (ROIs) along the brain's visual pathway. The T1 image was used to place the left and right optic nerves (ON) and the optic chiasm (OC) by gross anatomy. 4-mm spheres were used for the optic nerves (centered slightly posterior to the optic nerve head at the back of the eye), and a 6-mm sphere was used for the optic chiasm.

Tractography: We derived visual pathways through probabilistic diffusion-weighted tractography using MRtrix2 (Brain Research Institute, Melbourne, Australia)[18-26]. Constrained spherical deconvolution (CSD) estimates were used to generate fibers between two ROI pairs, representing the left and right optic nerves (ON » OC). Whole-brain tractography was completed using an L_{max} of 6 with 50,000 seeds and a maximum of 500,000 fibers. A modified white-matter mask generated using mrVista was used to constrain fibers to the brain while still allowing CSDs to be fit within the nasal cavity, enabling detection of the optic nerves. Final pathways were restricted to fibers passing between the specified ROIs, omitting any spurious results.

Fiber Cleaning: Fiber groups were cleaned using the Automated Fiber Quantification (AFQ) toolkit (Stanford University)[27], followed by a quality assessment and manual cleaning as necessary. Fibers were overlaid on the anatomical T1 volume and any fibers that were found to be anatomically implausible were manually removed. Pathways from all 12 participants were

processed using the same automated cleaning parameters and were manually refined by the same operator. A sample of the optic nerves from a representative subject are shown (Figure 1).

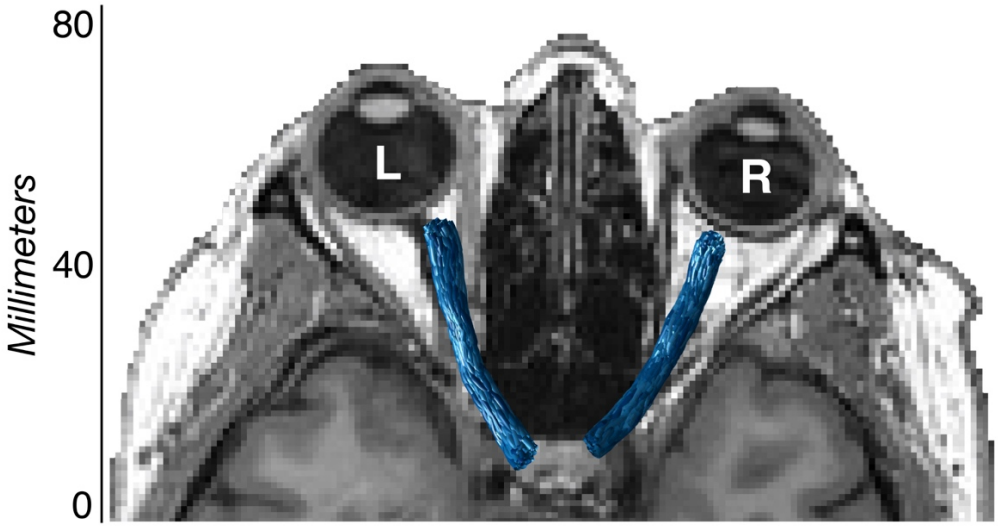

Figure 1. Visualization of final tractography-generated left and right optic nerve WM pathways (blue) in a representative glaucoma patient (G4).

Diffusion Measures: Voxel-wise tensor properties were extracted from the volumetric region defined by each tractography-generated pathway. The properties included in our analysis were mean diffusivity (MD, $\mu m^2/s$) and fractional anisotropy (FA). MD provides a measure of the diffusion of water molecules through tissue. It is useful as an approximation of white-matter density or myelination,[28] where large values indicate a diffuse ("weak") pathway, and small values indicate a denser and/or more myelinated ("strong") pathway. FA is highly sensitive to microstructural changes,[29] and provides a measure of diffusion directionality that is useful in approximating the structural integrity of a pathway, where large values indicate a single highly myelinated "intact" pathway, and small values indicate multiple intersecting, degenerated, or de-myelinated pathways. A sample of the MD and FA properties along the length of the optic nerves is shown in a representative patient with unilateral glaucoma (Figure 2).

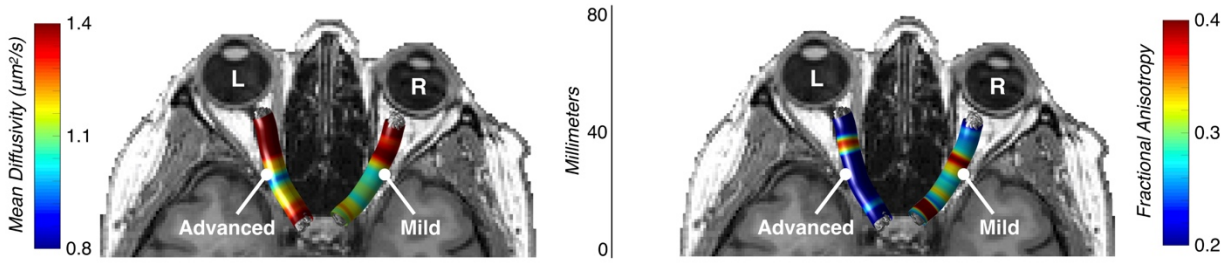

Figure 2. Mean diffusivity and fractional anisotropy values overlaid on the optic nerves of a representative glaucoma patient (G4). Mean diffusivity ($\mu m^2/s$) left and fractional anisotropy right.

Analysis: A combination of within- and between-groups analyses were conducted to evaluate the structural white-matter changes associated with glaucoma-related vision damage. All six asymmetric glaucoma patients had one eye with no or early glaucomatous defects ("mild") and one eye with moderate or advanced glaucomatous visual field loss ("advanced")[30]. Within-subjects, diffusion-tensor properties were compared between the "advanced" and "mild" eyes. Between-subjects, the ratios of "advanced" / "mild" optic nerve properties (FA) in glaucoma patients were compared to non-dominant/dominant ratios in controls.

To facilitate these comparisons and normalize pathway lengths, 100 samples were taken along the length of each pathway, such that 100 average MD and FA values were available for each pathway in each group (glaucoma or control). These values were generated for each cross-section using a Gaussian-weighted average, where the calculated "core" of each pathway was selectively weighted over the outlying fibers. From these 100 samples, the central eighty were retained for further analysis to reduce the risk of including measures contaminated by retinal cell bodies or contralateral fiber tracts. The central 80% of each sample was further subdivided into 10% bins to more precisely quantify differences along the pathway length.

Statistics: A linear mixed effect (LME) model was used to compare the MD and FA values of the advanced and mild optic nerves across the middle 80% and at each of the eight 10% bins in glaucoma patients. This model factored group (advanced or mild) as a fixed effect and subject as a random effect. Reported p-values are from ANOVAs of the fixed "Group" effects. The same LME model was used in the glaucoma and control ratio comparisons, as well as in all correlational data (factoring clinical/neurological measures as fixed effects and subjects as random effects).

Results

Selection of Clinical Measures of Structure and Function

As expected, we identified strong correlations between vCD and RNFL ($F(1,10) = 229.17$, $p = 3.20e\text{-}8$), vCD and VFI ($F(1,10) = 15.662$, $p = 0.0027$), and RNFL and VFI ($F(1,10) = 24.228$, $p = 0.00060$) (Figure 3). Because of the strong correlation between these clinical measures, we selected vCD and VFI as the main measurements of interest to evaluate for correlations with dMRI measures. These two measures are widely-used clinically for the evaluation of structural and functional glaucomatous damage.

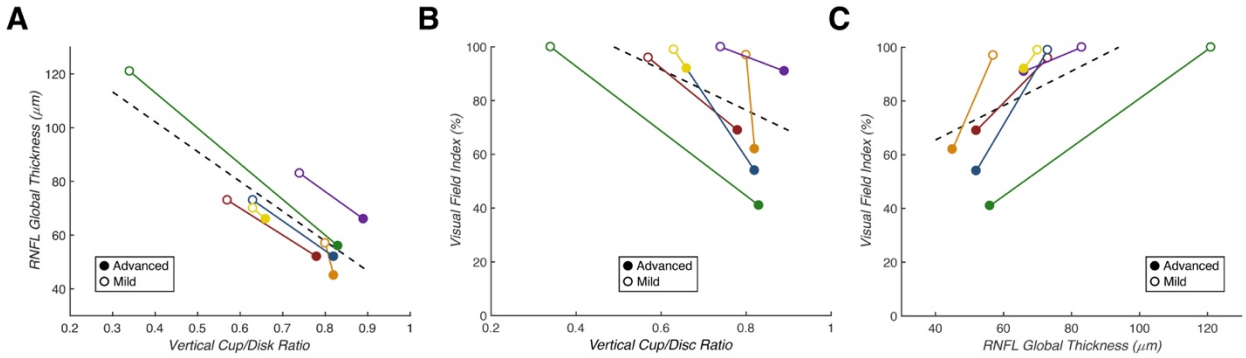

Figure 3. Summary of clinical measure correlations in glaucoma subjects. A: vCD predicts RNFL ($p = 3.20e\text{-}8$). B: vCD predicts VFI ($p = 0.0027$). C: RNFL predicts VFI ($p = 0.00060$). Subjects are indicated by color, with each point representing one eye. Closed points mark eyes with "advanced" glaucoma, while open points mark eyes with "mild" glaucoma. A least-squares regression estimate of the included values is indicated by the dashed line.

Diffusion Magnetic Resonance Imaging

Optic nerve white-matter pathways were successfully identified and refined in 6/6 glaucoma subjects and 6/6 controls. All pathways appeared to be anatomically correct after cleaning and were amenable to within-subjects and group-wise comparisons.

A significant difference in mean fractional anisotropy of the advanced and mild optic nerves of glaucoma subjects was noted in 3/8 bins ($F_1(1,10) = 55.442$, $p_1 = 2.20e\text{-}5$; $F_2(1,10) = 18.382$, $p_2 = 0.0016$; $F_3(1,10) = 11.322$, $p_3 = 0.0072$), along with a significant difference across the middle 80% ($F(1,10) = 55.474$, $p = 2.19e\text{-}5$) (Figure 4). In the same pathway, a significant difference in average mean diffusivity was noted in 1/8 bins ($F(1,10) = 10.885$, $p = 0.0080$).

Subsequent analyses focus on optic nerve fractional anisotropy because of the more reliable effect noted here (compared to MD).

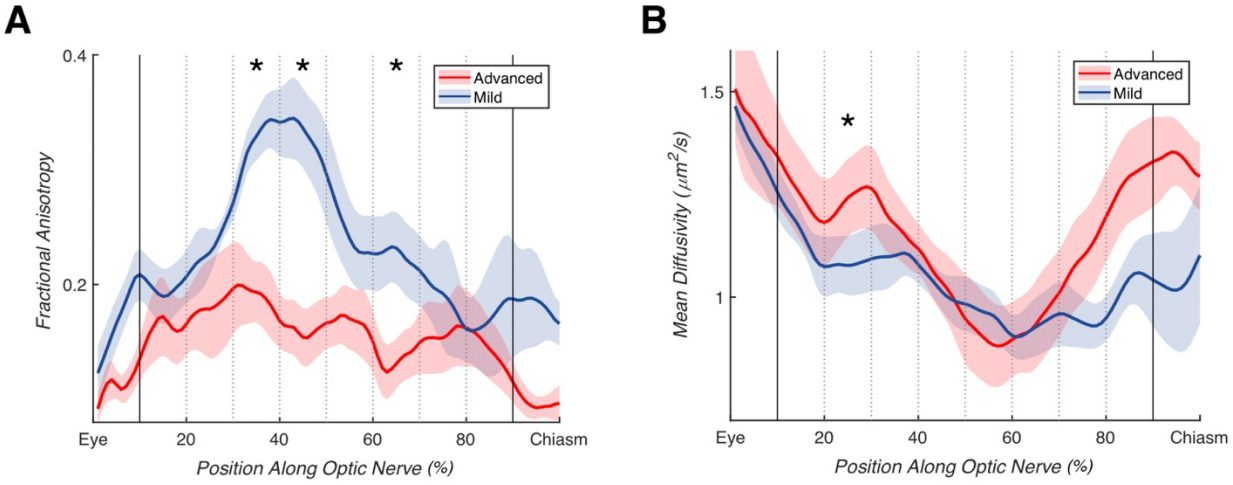

Figure 4. Tract profiles for the optic nerves of eyes with advanced (red) and mild (blue) glaucoma, with the middle 80% marked by bold lines, and each 10% bin with dotted lines. Significant differences ($p<0.05$) denoted by *. A: Significant differences in fractional anisotropy across the middle 80% ($p = 2.19e-5$), and in 3/8 individual bins ($p_1 = 2.20e-5$; $p_2 = 0.0016$; $p_3 = 0.0072$). B: Significant difference in mean diffusivity in 1/8 bins ($p = 0.0080$).

To more precisely characterize the nature of these within-subject effects, we compared the fractional anisotropy ratios of advanced/mild optic nerves in glaucoma subjects to non-dominant/dominant optic nerves in controls. This comparison exhibited selective FA reductions in the "advanced" optic nerves of glaucoma subjects, resulting in ratios <100%. As expected, no clear differences between non-dominant and dominant optic nerve FA values were noted in control subjects, with ratios around 100%. We found a significant difference between the optic nerve FA ratios of glaucoma subjects compared to controls in a LME model including group and age as fixed factors ($F(1,9) = 20.276$, $p = 0.0015$) (Figure 5).

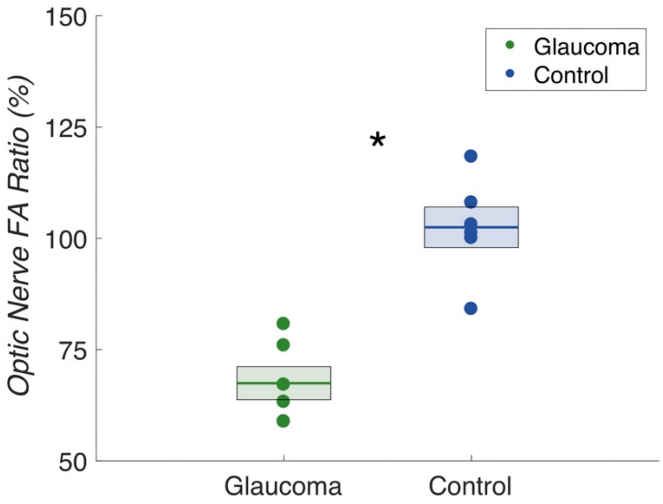

Figure 5. Comparison of optic nerve fractional anisotropy (FA) ratios (%) in glaucoma subjects (green) and controls (blue). Glaucoma subject ratios were calculated for "advanced" / "mild" ON FA, and control subject ratios were calculated for non-dominant/dominant ON FA. Mean ratios are indicated by the bold lines, with standard error denoted by the surrounding shaded region. Significant differences were found between FA ratios of glaucoma subjects and controls (p = 0.0015).

Relating dMRI with Clinical Measures in Glaucoma

We investigated the relationship between retinal, neural, and perceptual measures of glaucoma, correlating vCD, optic nerve FA, and VFI. We found that vCD predicted ON FA ($F(1,10) = 11.061$, $p = 0.0077$), and ON FA predicted the VFI ($F(1,10) = 15.308$, $p = 0.0029$) (Figure 6). Thus, reductions in ON FA link the retinal and perceptual impairments in glaucoma.

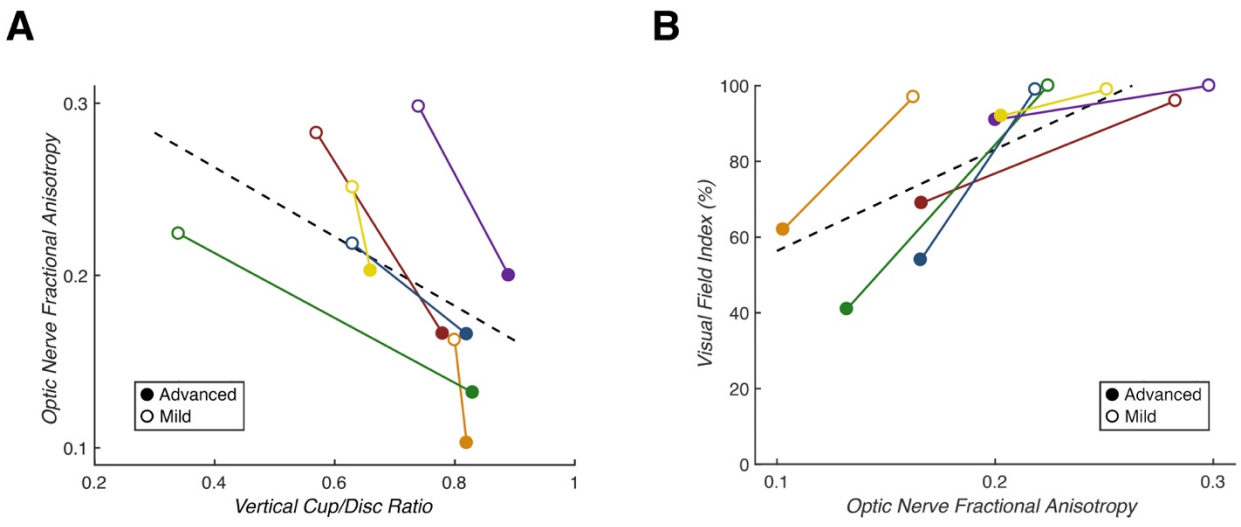

Figure 6. Summary of clinical and dMRI measure correlations in glaucoma subjects. A. vCD predicts ON FA ($p = 0.0077$). B. ON FA predicts VFI ($p = 0.0029$). Subject indicated by color, with each point representing one eye. Closed points mark eyes with "advanced" glaucoma, while open points mark eyes with "mild" glaucoma. A least-squares regression estimate of the included values is indicated by the dashed line.

Discussion

In this study, we assessed the feasibility of using probabilistic DWI tractography to examine the relationship between retinal, neural, and perceptual indices of optic nerve damage in patients with glaucoma. Using a 2-scan approach, we created combined (AP and PA) field-corrected DTI volumes that were used to successfully isolate optic nerve white matter pathways in 6/6 glaucoma subjects and 6/6 controls. The implementation of this adapted DWI methodology in a diverse patient pool (aged 19-66 years) with varying stages of disease severity validates its flexibility and investigative utility. To our knowledge, this is the first probabilistic tractography study to successfully isolate the optic nerves in glaucoma subjects. Additionally, we relate clinical measures of optic nerve structure and function (e.g. vCD and VFI) and dMRI measures of optic nerve integrity.

Comparing the structural properties of the optic nerves in glaucoma subjects, we noted significant differences in average mean diffusivity and fractional anisotropy of the "advanced" versus "mild" optic nerves. Overall, these trends (greater MD and smaller FA in "advanced" optic nerves) indicate disruption of the early visual system from glaucoma. These changes likely reflect neural changes from neurodegeneration at the level of the retinal ganglion cells. Additionally, through ratio comparison to control subjects, we demonstrated that these were not global changes in the optic nerves of glaucoma patients, but rather were unilateral changes in the "advanced" eyes.

Lastly, we examined the correlation between clinical ophthalmologic measures (vCD and VFI) and dMRI measures (optic nerve FA). We found that vCD was highly correlated with optic nerve FA, and that optic nerve FA was predictive of VFI. Thus, this analysis demonstrates an association between measures of glaucoma-related damage across three diagnostic modalities: retinal (vCD), neural (ON FA), and perceptual (VFI) measures.

The results of this study are highly significant, despite our limited sample size. Thus, this study validates the usefulness of probabilistic tractography as a means of evaluating structural differences in the visual pathways of glaucoma subjects. More interestingly, our exploration of the association between clinical measures of glaucoma and MRI-based data raises the exciting possibility of neuroimaging as a diagnostic tool. Optic nerve fractional anisotropy appears highly sensitive to glaucoma-related damage and may serve as a confirmatory or early diagnostic tool to detect microstructural glaucomatous aberrations in the optic nerves. Future studies evaluating subjects with earlier-stage glaucomatous disease and comparison to those with non-glaucomatous causes of optic neuropathy will allow for the assessment of MRI as a possible clinical tool for detecting and tracking the progression of visual disorders and other neurodegenerative diseases. MRI-based testing may provide a neurological marker of optic nerve damage, potentially enabling earlier diagnoses and improving treatment outcomes.

There is a need for larger follow-up studies assessing the correlation between these neural properties and clinical measures longitudinally over the course of disease progression. Such research may help inform future diagnostic and monitoring methods for glaucoma, as well as other visual and neurodegenerative disorders, potentially leading to improved prognosis and quality of life among patients affected by these conditions.

References

1. Welp A, Woodbury RB, McCoy MA, et al., editors. Making Eye Health a Population Health Imperative: Vision for Tomorrow. National Academies of Sciences, Engineering, and Medicine; Washington (DC): National Academies Press (US); 2016 Sep 15. 3, The Impact of Vision Loss.
2. Vu, H. T. V., Keeffe, J. E., McCarty, C. A., & Taylor, H. R. (2005). Impact of unilateral and bilateral vision loss on quality of life. *The British Journal of Ophthalmology, 89*(3), 360-363.
3. Quigley, H. A., & Broman, A. T. (2006). The number of people with glaucoma worldwide in 2010 and 2020. *British Journal of Ophthalmology, 90*(3), 262-267.

4. Davis, B. M., Crawley, L., Pahlitzsch, M., Javaid, F., & Cordeiro, M. F. (2016). Glaucoma: the retina and beyond. *Acta Neuropathologica, 132*(6), 807-826.

5. Leske, M. C. (2007). Open-angle glaucoma - An epidemiologic overview. *Ophthalmic Epidemiology, 14*(4), 166-172.

6. Jindal, V. (2013). Glaucoma: An Extension of Various Chronic Neurodegenerative Disorders. *Molecular Neurobiology, 48*(1), 186-189.

7. Engelhorn, T., Michelson, G., Waerntges, S., Struffert, T., Haider, S., & Doerfler, A. (2011). Diffusion Tensor Imaging Detects Rarefaction of Optic Radiation in Glaucoma Patients. *Academic Radiology, 18*(6), 764-769.

8. Frezzotti, P., Giorgio, A., Toto, F., De Leucio, A., & De Stefano, N. (2016). Early changes of brain connectivity in primary open angle glaucoma. *37*(12), 4581-4596.

9. Zikou, A. K., Kitsos, G., Tzarouchi, L. C., Astrakas, L., Alexiou, G. A., & Argyropoulou, M. I. (2012). Voxel-Based Morphometry and Diffusion Tensor Imaging of the Optic Pathway in Primary Open-Angle Glaucoma: A Preliminary Study. *American Journal of Neuroradiology, 33*(1), 128-134.

10. Gupta, N., & Yucel, Y. H. (2007). Glaucoma as a neurodegenerative disease. *Curr Opin Ophthalmol, 18*(2), 110-114.

11. Song, S.-K., Sun, S.-W., Ju, W.-K., Lin, S.-J., Cross, A. H., & Neufeld, A. H. (2003). Diffusion tensor imaging detects and differentiates axon and myelin degeneration in mouse optic nerve after retinal ischemia. *NeuroImage, 20*(3), 1714-1722.

12. Xu, J., Sun, S.-W., Naismith, R. T., Snyder, A. Z., Cross, A. H., & Song, S.-K. (2008). Assessing Optic Nerve Pathology with Diffusion MRI: from Mouse to Human. *NMR in biomedicine, 21*(9), 928-940.

13. Allen, Brian, Spiegel, Daniel P., Thompson, Benjamin, Pestilli, Franco, & Rokers, Bas. (2015). Altered white matter in early visual pathways of humans with amblyopia. *Vision Research, 114*, 48-55.

14. Allen, B., Schmitt, M. A., Kushner, B. J., & Rokers, B. (2018). Retinothalamic White Matter Abnormalities in Amblyopia. *Invest Ophthalmol Vis Sci, 59*(2), 921-929.

15. Andersson, J. L., Skare, S., & Ashburner, J. (2003). How to correct susceptibility distortions in spin-echo echo-planar images: application to diffusion tensor imaging. *Neuroimage, 20*(2), 870-888.

16. Smith, S. M., Jenkinson, M., Woolrich, M. W., Beckmann, C. F., Behrens, T. E., Johansen-Berg, H., et al. (2004). Advances in functional and structural MR image analysis and implementation as FSL. *Neuroimage, 23 Suppl 1*, S208-219.

17. Basser, P. J., Mattiello, J., & Lebihan, D. (1994). Estimation of the Effective Self-Diffusion Tensor from the NMR Spin Echo. *Journal of Magnetic Resonance, Series B, 103*(3), 247-254.

18. Basser, P. J., & Jones, D. K. (2002). Diffusion-tensor MRI: theory, experimental design and data analysis - a technical review. *NMR Biomed, 15*(7-8), 456-467.

19. Behrens, T. E., Woolrich, M. W., Jenkinson, M., Johansen-Berg, H., Nunes, R. G., Clare, S., et al. (2003). Characterization and propagation of uncertainty in diffusion-weighted MR imaging. *Magn Reson Med, 50*(5), 1077-1088.

20. Calamante, F., Tournier, J. D., Jackson, G. D., & Connelly, A. (2010). Track-density imaging (TDI): super-resolution white matter imaging using whole-brain track-density mapping. *Neuroimage, 53*(4), 1233-1243.

21. Conturo, T. E., Lori, N. F., Cull, T. S., Akbudak, E., Snyder, A. Z., Shimony, J. S., et al. (1999). Tracking neuronal fiber pathways in the living human brain. *Proc Natl Acad Sci U S A, 96*(18), 10422-10427.

22. Mori, S., & van Zijl, P. C. (2002). Fiber tracking: principles and strategies - a technical review. *NMR Biomed, 15*(7-8), 468-480.

23. Parker, G. J., Haroon, H. A., & Wheeler-Kingshott, C. A. (2003). A framework for a streamline-based probabilistic index of connectivity (PICo) using a structural interpretation of MRI diffusion measurements. *J Magn Reson Imaging, 18*(2), 242-254.

24. Tournier, J. D., Calamante, F., & Connelly, A. (2007). Robust determination of the fibre orientation distribution in diffusion MRI: non-negativity constrained super-resolved spherical deconvolution. *Neuroimage, 35*(4), 1459-1472.

25. Tournier, J. D., Calamante, F., & Connelly, A. (2012). MRtrix: Diffusion tractography in crossing fiber regions. *22*(1), 53-66.

26. Tournier, J. D., Calamante, F., Gadian, D. G., & Connelly, A. (2004). Direct estimation of the fiber orientation density function from diffusion-weighted MRI data using spherical deconvolution. *Neuroimage, 23*(3), 1176-1185.

27. Yeatman, J. D., Dougherty, R. F., Myall, N. J., Wandell, B. A., & Feldman, H. M. (2012). Tract Profiles of White Matter Properties: Automating Fiber-Tract Quantification. *PLOS ONE, 7*(11), e49790.

28. Alexander, A. L., Hurley, S. A., Samsonov, A. A., Adluru, N., Hosseinbor, A. P., Mossahebi, P., et al. (2011). Characterization of cerebral white matter properties using quantitative magnetic resonance imaging stains. *Brain Connect, 1*(6), 423-446.

29. Malania, M., Konrad, J., Jagle, H., Werner, J. S., & Greenlee, M. W. (2017). Compromised Integrity of Central Visual Pathways in Patients With Macular Degeneration. *Invest Ophthalmol Vis Sci, 58*(7), 2939-2947.

30. "Glaucoma ICD-10 Quick Reference Guide." *ICD-10-CM*, American Academy of Ophthalmology, 29 Aug. 2017, www.aao.org/Assets/5adb14a6-7e5d-42ea-af51-3db772c4b0c2/636396205914600000/glaucoma-quick-reference-guide-update-8-29-17-pdf?inline=1.